



Impact of scapular notching on glenoid fixation in reverse total shoulder arthroplasty: an in vitro and finite element study

Min Zhang, PhD^{a,b,*}, Sarah Junaid, PhD^{b,c}, Thomas Gregory, MD^{b,d},
Ulrich Hansen, PhD^b, Cheng-Kung Cheng, PhD^a

^aBeijing Advanced Innovation Centre for Biomedical Engineering and School of Biological Science and Medical Engineering, Beihang University, Beijing, China

^bMechanical Engineering Department, Imperial College London, London, UK

^cEngineering and Applied Sciences, Aston University, Birmingham, UK

^dDepartment of Orthopaedic Surgery, Avicenne Teaching Hospital, APHP, University Paris XIII, Bobigny, France

Background: The high incidence of scapular notching in reverse total shoulder arthroplasty (RTSA) has spurred several methods to minimize bone loss. However, up to 93% of RTSAs accompanying scapular notching have been reported to maintain good implant stability for over 10 years. This study was conducted to investigate the relationship between scapular notching and glenoid fixation in RTSA.

Methods: Cadaveric testing was performed to measure the notch-induced variations in strain on the scapular surface and micromotion at the bone-prosthesis interface during arm abductions of 30°, 60°, and 90°. Finite element analysis was used to further study the bone and screw stresses as well as the bone-prosthesis micromotion in cases with a grade 4 notch during complicated arm motions.

Results: The notch resulted in an apparent increase in inferior screw stress in the root of the screw cap and at the notch-screw conjunction. However, the maximum stress (172 MPa) along the screw after notching is still much less than the fatigue strength of the titanium screw (600 MPa) under cyclic loading. The bone-prosthesis micromotion results did not present significant notch-induced variations.

Conclusions: Scapular notching will lead to few impacts on the stability of an RTSA on the glenoid side. This finding may explain the long-term longevity of RTSA in cases of severe scapular notching. The relationship between scapular notching and weak regions along the inferior screw may explain why fractures of the inferior screw are sometimes reported in patients with RTSA clinically.

Level of evidence: Basic Science Study; Biomechanics and Computer Modeling

© 2020 Journal of Shoulder and Elbow Surgery Board of Trustees. All rights reserved.

Keywords: Scapular notching; reverse total shoulder arthroplasty; in vitro testing; finite element analysis; fixation; micromotion

Institutional Review Board approval was received from the Imperial College Research Ethics Committee.

*Reprint requests: Min Zhang, PhD, Beihang University, No. 37 Xueyuan Road, Haidian District, Beijing, China 100083.

E-mail address: zhangminsky123@msn.com (M. Zhang).

Scapular notching is a result of mechanical impingement between the humeral cup and the scapular neck, which often leads to implant wearing and the generation of polyethylene debris. The polyethylene particles can

trigger osteolytic reactions and further enlarge the bone notch. Scapular notching is a frequently reported complication of Grammont reverse total shoulder arthroplasty (RTSA), occurring in 44%-93% of patients.^{6,8,10,12} Notching can appear within the first few postoperative months of a patient undergoing RTSA and may continue to progress over time.^{6,12,16} This condition is also sometimes accompanied by screw fracture and implant loosening.^{7,26} Thus, the presence of scapular notching has long been a clinical concern,^{2,7,26} and numerous publications have reported on efforts to minimize bone-prosthesis impingement and scapular notching.^{5,19,24} However, a recent review of RTSA longevity studies reported that the postoperative survivorship of RTSA is 70% at 15 years; when prosthesis failure alone is viewed as the reason for revision, the survivorship rate reaches 85% at 15 years.⁶ Moreover, at a follow-up of 10 or more years, 93% of patients with RTSA had scapular notching, 48% of whom had grade 3 or 4.⁶ It is not yet clear whether scapular notching is associated with implant survivorship, particularly whether severe notching promotes aseptic glenoid loosening, which has been reported in 12% of Grammont RTSAs.²

Previous studies on the fixation strength of the glenoid baseplate in RTSA included in vitro testing and finite element analysis (FEA). In vitro testing can closely replicate the conditions in the body, but the range of arm motions is restricted and this method can provide only limited information on what is happening within the joint. Roche et al²⁴ used an in vitro setup to evaluate initial implant fixation through bone-prosthesis micromotion after scapular notching. However, only arm abduction was simulated. FEA can simulate any joint movement through a range of complicated activities and is beneficial for assessing stresses and forces that cannot be easily measured using other means.

This study aimed to use an in vitro setup and FEA to quantitatively assess the correlation between scapular notching and glenoid fixation in RTSA. The fixation was assessed according to initial implant stability and screw stability. Cadaveric testing was performed to investigate the notch-induced variations in the strain on the scapular surface and bone-prosthesis micromotion under 30°, 60°, and 90° of humeral abduction, respectively. For more complex shoulder movements (lifting an object to head height and standing up from an armchair), FEA was used to further study the effect of scapular notching on the stability of the glenoid component in RTSA regarding screw safety, screw stability, and initial implant stability with the parameters of screw stress, bone stress on the surface of the screw hole, and bone-prosthesis micromotion. Given the high incidence of scapular notching but low revision rates for RTSA, it was hypothesized that a grade 4 scapular notch would have little effect on the stability of RTSA during the simulated daily activities.

Materials and methods

This study aimed to assess the effect of scapular notching on glenoid fixation by using in vitro testing and FEA. The detailed study process is presented.

In vitro testing

Three cadaveric scapulae (International Institute for the Advancement of Medicine, Edison, NJ, USA) without any history of shoulder disease or surgery were used for the in vitro evaluation (Table I). The method for preparing the cadaveric scapulae for testing was described in a previous publication by Zhang.³⁰ The cadaveric shoulders, which were stored in a -20°C freezer, were thawed at room temperature the night before in vitro testing began. Then, the scapula was separated from each shoulder, and all the soft tissues on the surface of each scapula were cleared out. Bone strains on the scapular surface and bone-prosthesis micromotions in both the un-notched and notched conditions were measured with the aim of evaluating the effect of scapular notching on implant stability. Methods for preparing to measure these 2 parameters on in vitro testing are described in the following subsections.

Preparation for measuring bone strains on scapular surface

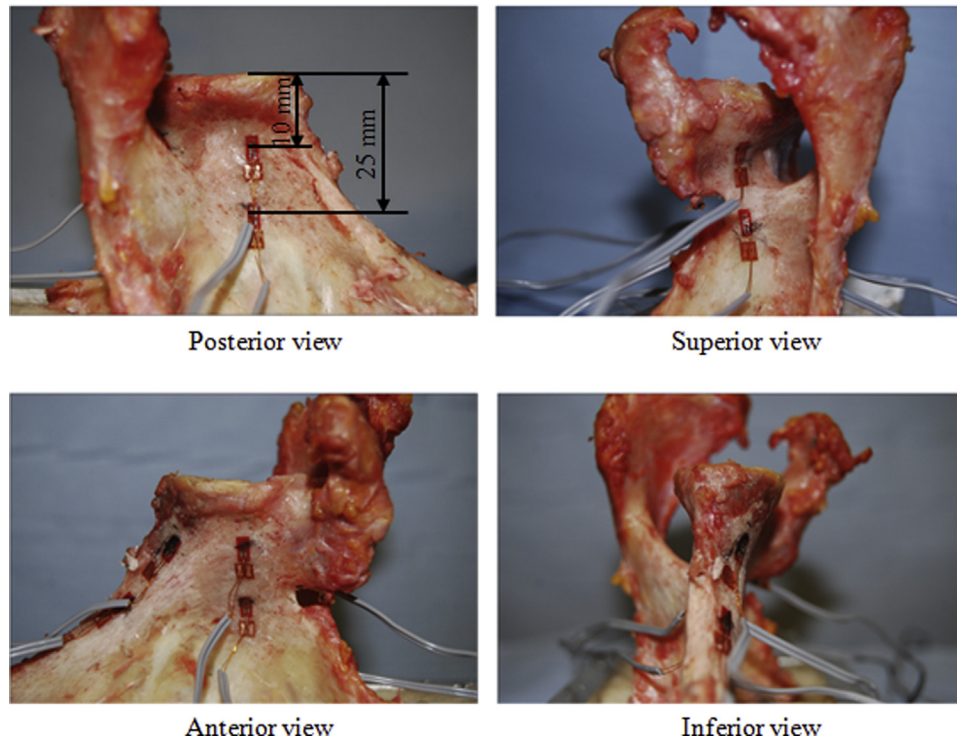
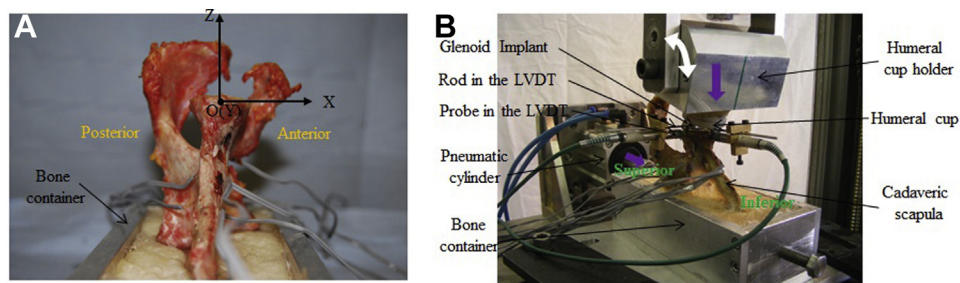
On each scapula, 8 uniaxial strain gauges (FLA-2-11; Tokyo Sokki Kenkyujo, Tokyo, Japan) were attached at approximately 10 mm and 25 mm beneath the glenoid articular surface and around the glenoid at each level (Fig. 1). These 2 levels were chosen with the purpose of investigating strain close to, and at a small distance from, the glenoid. The strain gauges on the anterior, posterior, and superior surfaces of the scapula were roughly perpendicular to the glenoid articular surface. The strain gauges located on the inferior surface were orientated parallel to the lateral border. The procedure of fixing a strain gauge on the bone surface conformed to the method introduced by Dabestani.¹⁸ The location where a strain gauge would be attached was first specified and marked with a black permanent marker. Then, the bone surface at the target location was cleared of periosteum and abraded with 400-grit silicon-carbide paper. Finally, as suggested by Wright and Hayes,²⁹ 1 strain gauge was attached to the bone surface with M-Bond 200 adhesive (Vishay Measurements Group, Basingstoke, UK). All the strain gauges on the surface of each scapula were connected to a calibrated model P3 strain recorder (accuracy, 1 µε; Vishay Measurements Group) for strain measurements.

Setup of bone-prosthesis interface micromotion test

As shown in Figure 2, A, one-third of each scapula on the medial side was secured in a container filled with polymethyl methacrylate bone cement (Simplex; Stryker, Kalamazoo, MI, USA). The coordinate system (Fig. 2, A) was defined in accordance with the system proposed by Terrier et al,²⁷ with the middle point of the glenoid fossa being the origin (O) of the coordinate system. The x-axis was orientated from posterior to anterior, the y-axis was orientated from inferior to superior, and the z-axis was defined as being perpendicular to the glenoid articular surface. An experienced orthopedic shoulder surgeon implanted

Table I Characteristics of cadaveric scapulae

Subject No.	Sex	Age, yr	Side	No. of voxels	Voxel size, mm
1	Female	70	Right	512 × 512 × 507	0.56 × 0.56 × 0.33
2	Male	66	Right	512 × 512 × 788	0.85 × 0.85 × 0.33
3	Female	71	Left	512 × 512 × 533	0.48 × 0.48 × 0.33

**Figure 1** Positions of strain gauges on cadaveric scapula surface.**Figure 2** Experimental setup. (A) Inferior view of scapula settled in bone container. (B) Setup of in vitro testing. LVDT, linear variable differential transformer.

each shoulder joint with a Delta CTA RTSA (DePuy Synthes, Warsaw, IN, USA) using the procedure detailed in the 2005 version of the Delta implant surgical guide (DePuy Synthes). The relative movement (micromotion) at the bone-prosthesis interface was measured using a linear variable differential transformer (LVDT) (DP/2/S; Solartron Metrology, Bognor Regis, UK) (resolution, 0.01 μm) (Fig. 2, B). Four calibrated LVDTs were fixed to the superior, inferior, anterior, and posterior of the metal glenoid implant.

Measurement in un-notched bone condition

All the scapulae with the strain gauges and RTSA were first used for measurements in the un-notched bone condition. The test setup is shown in Figure 2, B. The bone container holding the un-notched scapula was secured on the platform of a tensile testing machine (Instron, Norwood, MA, USA). The superoinferior direction of the scapula was aligned with the matching humeral cup (DePuy Synthes) and the pneumatic cylinder. The humeral cup was fixed to the actuator in the Instron machine and supplied the

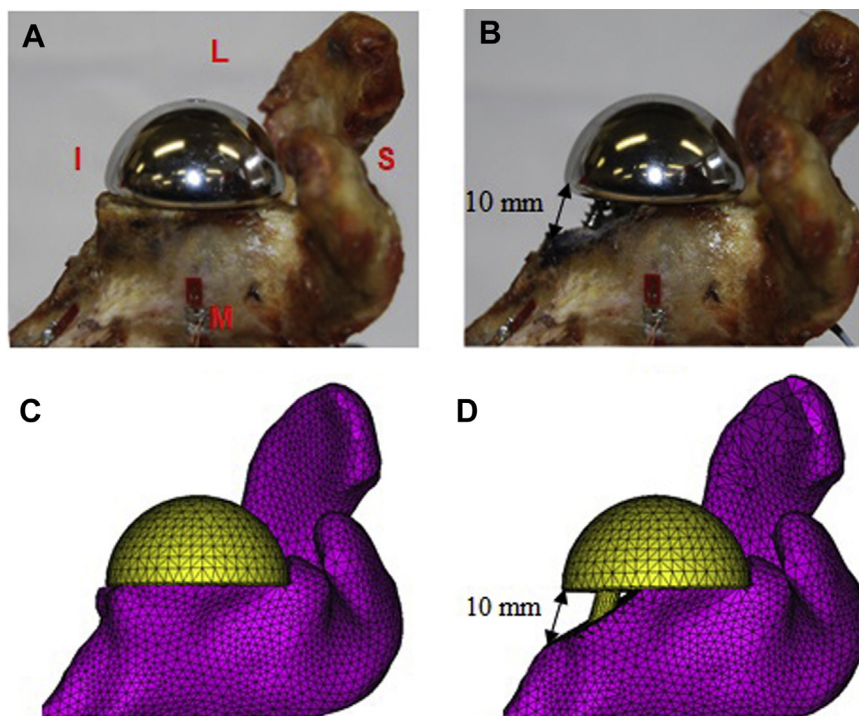


Figure 3 Implanted scapulae with and without grade 4 notch. (A) Implanted cadaveric scapula without notch from anterior view. (B) Implanted cadaveric scapula with inferior notch. (C) Finite element model of implanted scapula without notch. (D) Finite element model of implanted scapula with inferior notch. *L*, lateral; *I*, inferior; *S*, superior; *M*, medial.

vertical force. The pneumatic cylinder was fixed with the platform of the Instron machine and applied the horizontal force. The maximum glenohumeral force values in the arm motions of 30°, 60°, and 90° of abduction were obtained from the study of Terrier et al²⁷ (Supplementary Appendix S1). The strain value measured by each strain gauge around the glenoid under each abduction angle was recorded. The output from each LVDT was also recorded. To reduce the effect of the viscoelastic properties of bone on the results, a 5-minute restoration period was allowed for each scapula before the start of the next loading case.⁴ Because of possible impingement between the rod for securing the inferior LVDT on the implant and the humeral cup at 30° and 60° of abduction, inferior micromotions under these 2 conditions were not recorded. The test was repeated 3 times for each abduction angle, and the average value was used to represent the strain and micromotion for that angle.

Measurement in notched bone condition

After all testing of un-notched samples was complete, a Nerot-Sirveaux grade 4 inferior artificial notch (Fig. 3, A) was handmade in each scapula by use of a saw, with the most medial border of the notch being roughly 10 mm below the inferior rim of the glenoid component.²⁵ The positioning of the notch was consistent with that reported in the clinical literature.^{21,26} The strain gauges used for testing on the un-notched scapulae remained in place during the notching procedure. Gauges that were broken or damaged were replaced with new gauges at the same positions. The operation methods for positioning the bone container on the Instron machine platform and force loading on the glenoid in the notched

condition were the same as those in the previous testing. Strains and micromotions around the glenoid were recorded and compared with the pre-notched results. A paired *t* test was used to investigate the effect of severe notching on bone strain and micromotion. $P < .05$ was considered statistically significant.

Analysis of effect of scapular notching on implant stability in daily activities with finite element modeling

Before further analysis of the effect of scapular notching on implant stability in complex daily activities with finite element (FE) modeling, the notch-induced changes in bone strain and bone-prosthesis micromotion with 30°, 60°, and 90° of arm abduction predicted from the finite element model (FEM) were validated with the results of the previous experiments. The believable FEM, which had been validated with the in vitro testing results, would be used for further study of daily activities.

Validation of FEM

The method of building the FEM of a scapula accompanied by a glenoid component in RTSA was described in our previous work³¹ and consists of the following steps: Computed tomography images of all 3 scapulae (Table I) were used to reconstruct the geometry of the bone via Avizo software (version 5; Mercury Systems, Andover, MA, USA). Each reconstructed scapula model was implanted with a Delta CTA RTSA with guidance from an experienced orthopedic shoulder surgeon and following the surgical

technique for this type of prosthesis (2005 revision; DePuy Synthes). The glenoid component and screw positions of each scapula in the FEM were consistent with those of the same bone in the previous cadaveric testing. Each FEM of an implanted scapula was used to create 2 models: with and without a scapular notch (Fig. 3, B). For each notched model, a Nerot-Sirveaux grade 4 notch²⁶ was simulated to be consistent with the notch created in the same cadaveric scapula. All the notched and un-notched FEMs were imported into MSC Marc software (MSC Software, Santa Ana, CA, USA) for FE pre-processing and modeling. Methods of FE modeling in MSC Marc for notched and un-notched bone were the same. Each model of bone with a Delta CTA RTSA was composed of isotropic and linear elastic tetrahedral elements. The material properties of each element in the FEM of the scapula were determined by the computed tomography values and the density-modulus relationship proposed by Carter and Hayes.³ The FEMs of the 3 cadaveric scapulae in the intact condition were validated against results from in vitro cadaveric testing in our previous work.³⁰ The Young modulus of the cobalt-chrome baseplate and the glenohumeral sphere was set as 210 GPa, and that of the titanium screws for securing the glenoid component was set as 110 GPa.¹⁴ The Poisson ratio for all the elements was 0.3. The bone-prosthesis interface was unbonded with a friction coefficient of 0.4,¹⁴ which has been shown to be consistent with in vitro conditions.¹³ The screws were assumed to provide firm fixation and thus to be rigidly bonded with the bone. The FEMs used the same coordinate system, arm abduction angles, and boundary conditions as in vitro testing. Similarly, the strain in the FEMs was recorded at the same points where the strain gauges were in the in vitro test and in the same direction as the gauge orientation. The relative movement between the glenoid baseplate and the position of the LVDT probe on the bone was also calculated. Convergence testing for each analyzed scapula showed that a mesh size of 1.5 mm in the region of the glenoid and 3.0 mm in the remaining bone was able to produce reliable strains and micromotions.³⁰ The FE notch-induced strain change in the position of each strain gauge from the 3 scapula models was averaged. In addition, the bone-prosthesis micromotion in each direction of the glenoid from the 3 subjects was averaged. Because of unavoidable differences between in vitro testing and the FEM in accordance with notch shape, implant position, and screw location, a comparison was made between in vitro testing and the FEM to assess the effect of scapular notching on strain and bone-prosthesis micromotion. This comparison was used to assess the accuracy of the FEM.

Effect of scapular notching on implant stability in daily activities

After validation of the FEMs as described earlier, the models were used to simulate 2 complicated shoulder movements: lifting a block (5 kg) to head height and standing up from an armchair. These 2 activities have been reported to produce the greatest glenohumeral contact forces and anteroposterior shear forces among 13 daily shoulder activities in patients with RTSA.¹⁵ The force values for these 2 activities presented by Kontaxis¹⁵ were used (Supplementary Appendix S1). Maximum principal stresses along the screws and on the surface of the screw holes, as well as bone-prosthesis micromotions, were evaluated. A paired *t* test was used to assess the effect of

scapular notching on the stability of the glenoid implant. $P < .05$ was considered statistically significant.

Results

In vitro testing

The strains recorded from each strain gauge from the 3 cadaveric scapulae were averaged and are presented in Figure 4, A and B. The presence of a notch did not lead to significant effects on the bone strains around the scapula during arm elevation ($P = .863$), whereas the magnitude of the strain changes varied depending on gauge location and activity being performed. The loading-dependent characteristic of notch-induced bone strain presents a necessity for more realistic and complicated loading simulations.

Mean bone-prosthesis interface micromotions in each LVDT position in the 3 subjects are presented in Figure 4, C. The notch did not significantly impact the bone-prosthesis relative movements around the glenoid component during arm elevation ($P = .843$).

Validation of FEM with experimental measurements

Notch-induced strain variations from the FEMs of the 3 subjects were averaged in each strain gauge position and are illustrated with the in vitro results in Figure 5. The FE results in the notch-induced strain variations around the glenoid displayed a trend consistent with those from the cadaveric scapula testing. Both the FE and experimental data presented an apparent decrease in notch-induced strain changes from the position close to the glenoid to that far away around the glenoid. The maximum difference between the FE notch-induced strain variation around the glenoid and that obtained from the experimental results was 14 $\mu\epsilon$ and occurred on the lateral-posterior glenoid surface.

The comparison between the FE and experimental micromotion variations indicated that the FEM of scapulae can predict the same levels of micromotion as in vitro testing ($P = .647$). The maximum FE-experimental difference in the notch-induced micromotion variations around the glenoid was 0.50 μm .

Effect of scapular notching on implant stability in daily activities

Distributions of the maximum principal stress along the inferior screw for the 3 subjects before and after notching were predicted with FEA. The result showed the same trend of stress distribution along the inferior screw for the 3 subjects. One subject's stress distributions when rising from an armchair are exhibited in Figure 6, A. The results indicated that high stresses appeared in the root of the screw cap. The scapular notch resulted in an increase in the

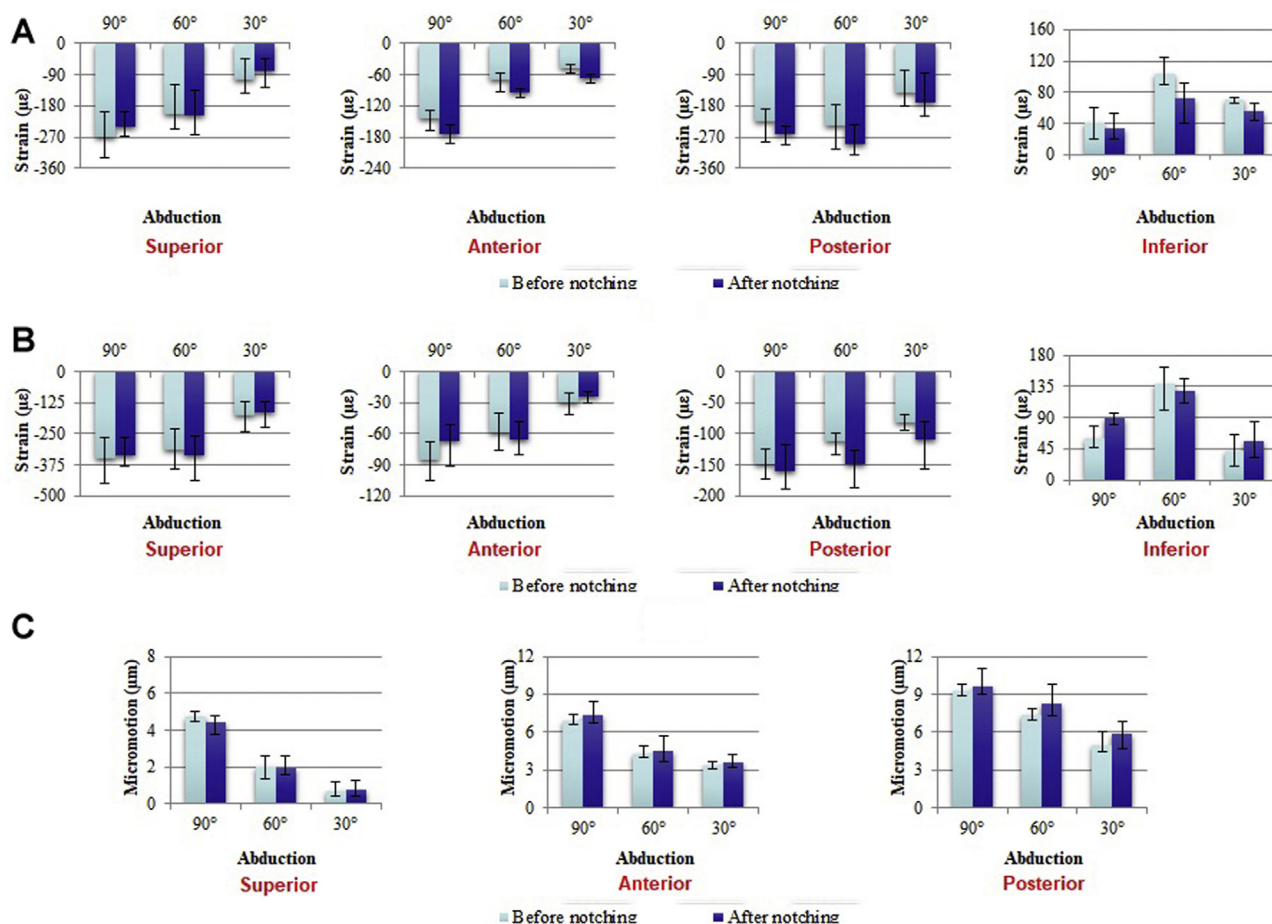


Figure 4 In vitro testing results. (A) Strains on glenoid surface at level approximately 10 mm medial to glenoid articular surface during various arm abductions before and after notching. (B) Strains on glenoid surface at level approximately 25 mm medial to glenoid articular surface during various arm abductions before and after notching. (C) Micromotion at bone-prosthesis interface around glenoid before and after notching.

maximum principal stress for all 3 subjects. The average maximum principal stresses of the 3 subjects in the case of a Nerot-Sirveaux grade 4 inferior notch reached 72.5 MPa (standard deviation [SD], 4.8 MPa) while lifting a block to head height and 172.0 MPa (SD, 6.2 MPa) while standing up from an armchair. When the notch-induced stress changes on each cross section along the screw at 2-mm intervals were averaged, all 3 subjects' results presented consistent trends in the 2 shoulder activities. One subject's results are illustrated in Figure 6, B. Both simulated arm activities led to an apparent notch-induced increase in stress in the root of the screw cap and at the conjunction between the notch and the inferior screw. Moreover, large glenohumeral contact force resulting from the activity of standing up from an armchair led to the most apparent increase in stress after scapular notching.

The distribution of the maximum principal stress on the surface of the inferior screw hole before and after notching was used to assess the possibility of notch-induced bone fracture. The results of all 3 subjects showed the same stress distribution. High stresses appeared close to the screw tip, as shown in Figure 7, which presents 1 subject's

stress distributions before and after scapular notching when standing up from an armchair. In addition, the bone stress on the surface of the screw hole was increased after scapular notching, with the mean maximum principal stress of the 3 subjects during the 2 simulated shoulder joint activities being 3.3 MPa (SD, 0.9 MPa).

Micromotion distributions at the bone-prosthesis interface in the 3 subjects before and after scapular notching were calculated. Figure 8 presents distributions of 1 subject's bone-prosthesis micromotion when rising from an armchair. The results showed no significant variations in bone-prosthesis micromotion ($P = .868$). The mean peak notch-induced increase in bone-prosthesis micromotion in the 3 subjects was 2.68 µm (SD, 0.57 µm) and occurred when standing up from an armchair.

Discussion

Both in vitro testing and FE analysis methods were used to investigate the effect of inferior scapular notching on glenoid fixation in RTSA. The most important findings are as

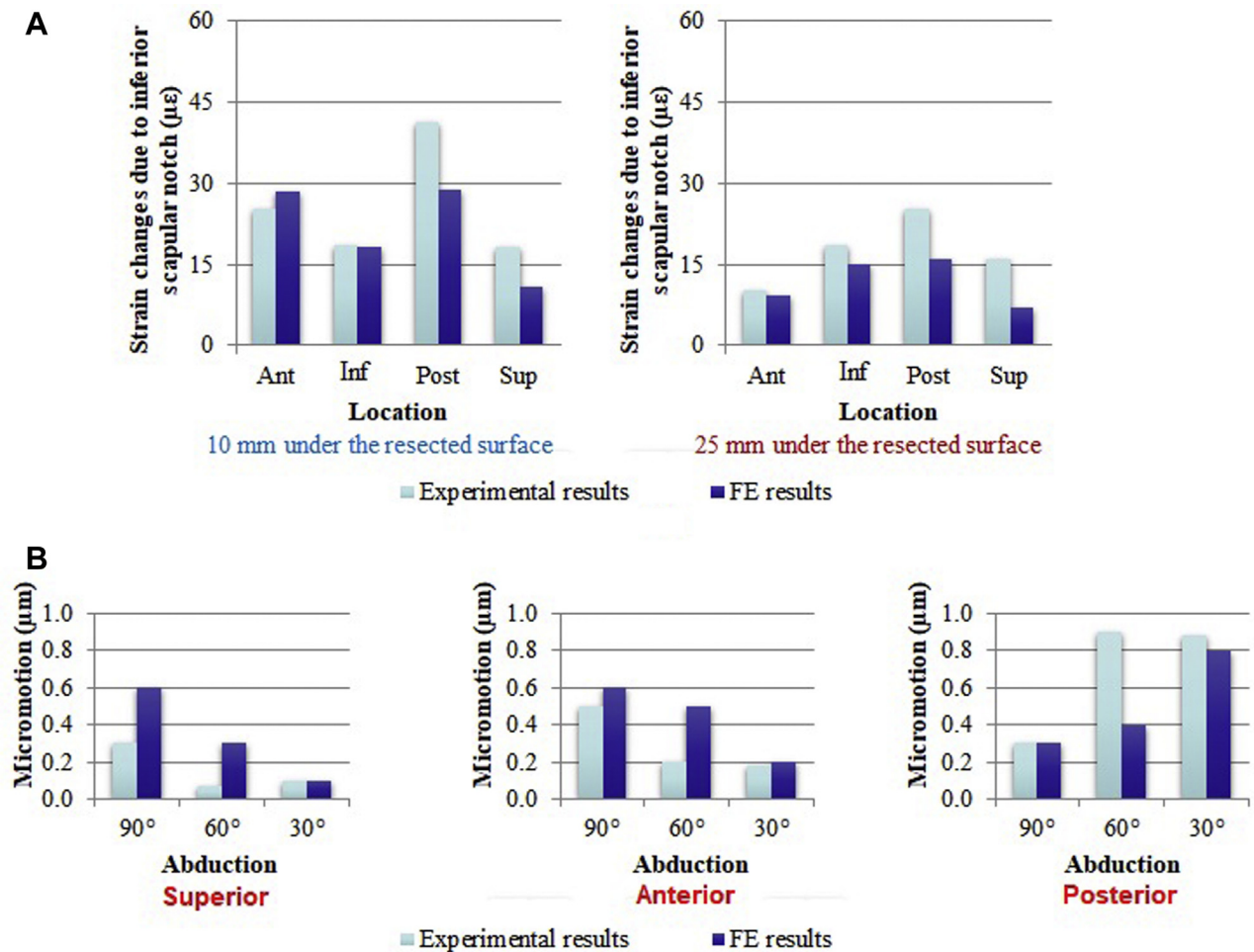


Figure 5 Finite element (FE)–experimental comparison. (A) Comparison between experimental and FE notch-induced strain variations around scapula. (B) Comparison between experimental and FE notch-induced micromotion variations around scapula during various arm abductions. *Ant*, anterior; *Inf*, inferior; *Post*, posterior; *Sup*, superior.

follows: (1) Notch-induced stress variation was loading and location dependent. (2) An inferior scapular notch led to an apparent increase in stress in the root of the screw cap, as well as at the screw-notch interface. (3) The bone stress on the surface of the screw hole increased in the presence of a scapular notch. (4) A severe inferior scapular notch resulted in few variations in micromotion at the bone-prosthesis interface during daily arm activities.

Strains on the surface of 3 cadaveric scapulae before and after scapular notching under 30°, 60°, and 90° of arm abduction were measured using in vitro testing. The results showed that notch-induced strain variation was loading and location dependent. The region close to the notch was generally impacted by the notch more than the region far from the notch. This possibly occurs because no bone supports the inferior screw in the region of bone loss and, thus, bone close to the notch incurred more stresses.

The FEM for predicting the strains and micromotions in the bone condition of an inferior scapular notch were validated with the completed in vitro testing. The maximum

deviation between the FE notch-induced strain variations and those from experiments was 14 µε. The maximum difference in the FE bone-prosthesis micromotion changes from the in vitro testing results was 0.50 µm. The FE-experimental variation could have been caused by the unavoidable inconsistent notch geometries, implant positions in the FEM and the experiments, and unavoidable differences induced by replacing the strain gauge broken by making a notch. The slight changes in the location of the glenoid component in RTSA and the notch surface created by hand may have led to variations in the force transmitted from the glenoid prosthesis to the bone. The unpredicted contact condition at the interface between the nonlocked screws (anterior and posterior screws in the Delta CTA RTSA) and the bone on in vitro testing is possibly another explanation for the FE-experimental variations. In the FEM, the nonlocked screws were assumed firmly secured. The real condition may not have been the same as the assumption in the FEM and may have led to different experimental results. However, the FEM of the 3 scapulae

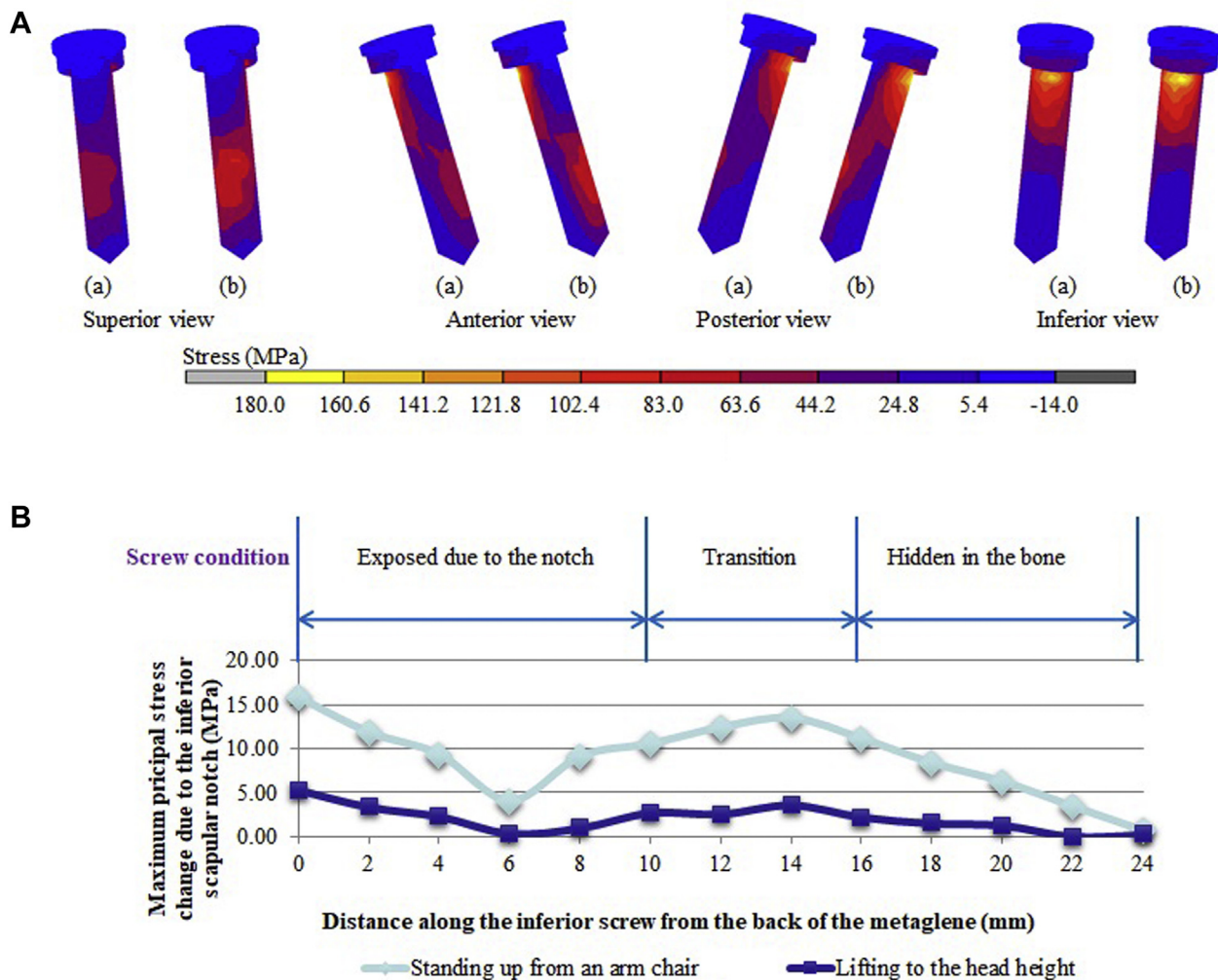


Figure 6 Maximum principal stresses on surface of inferior screw. (A) Distributions of maximum principal stresses on surface of inferior screw before (a) and after (b) scapular notching. (B) Variations in maximum principal stresses after notching along inferior screw from back of baseplate to screw tip.

when in the intact condition had been validated against the results of in vitro cadaveric testing in our previous work.³⁰ Moreover, the notch-induced strain variations predicted from the FEM displayed a trend consistent with those measured from in vitro testing under the same loading and fixation conditions. Thus, the FEM was able to predict believable strain variations induced by the inferior scapular notch. The maximum difference between the FE notch-induced micromotion changes and those from in vitro testing ($0.50 \mu\text{m}$) was much lower than the threshold for bone integration ($50 \mu\text{m}$)²²; thus, the FE-experimental difference will lead to few impacts on the prediction of bone ingrowth after RTSA implantation.

With the validated FEM of implanted scapulae, 2 complicated daily physical activities of the shoulder were simulated. The predicted notch-induced stress changes along the inferior screw depicted that a notch led to an apparent increase in screw stress in the root of the screw cap and at the screw-notch interface. The 2 regions of large

notch-induced stress variation predicted from the FEM are in line with the positions of screw fractures reported in clinical practice.^{11,26} The agreement between the FE results and the clinical observation indicated that the FEM of an implanted scapula with a scapular notch could predict believable results when the effects of severe notching on the inferior screw were analyzed. In this study, the predicted maximum principal stress of the inferior screw in the bone condition of a Nerot-Sirveaux grade 4 notch was 172 MPa and occurred when standing up from an armchair, which resulted in the largest glenohumeral joint contact force in the 13 daily arm activities reported by Kontaxis.¹⁵ This value was much smaller than the fatigue strength of the inferior titanium screw (600 MPa) in daily life.²⁸ It documented that the inferior screw in a scapula implanted with an RTSA was comparatively safe in the case of scapular notching. The incidence of breakage of the inferior screw accompanied by scapular notching in clinical practice was reported as 2% by Sirveaux et al²⁶ and as 1% by

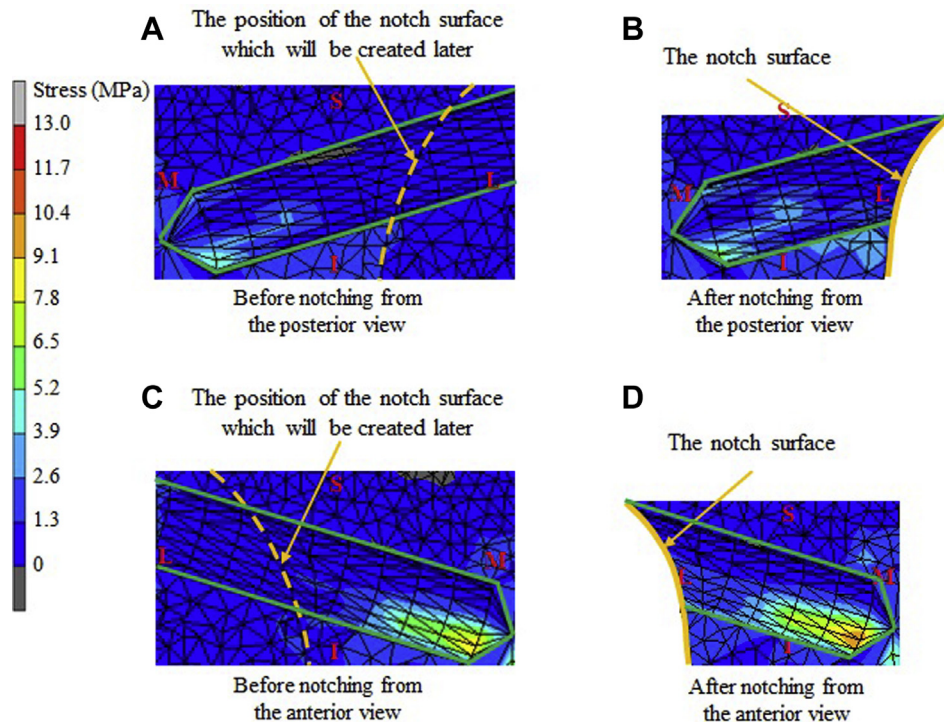


Figure 7 Distribution of maximum principal stresses on surface of inferior screw hole before and after scapular notching. (A) Intact inferior screw hole before scapular notching from posterior view. (B) Remaining inferior screw hole after scapular notching from posterior view. (C) Intact inferior screw hole before scapular notching from anterior view. (D) Remaining inferior screw hole after scapular notching from anterior view. The *green line* is the contour of the inferior screw hole. The *dashed yellow line* marked on each intact scapular neck image is the position of the notch surface that will be created later. The *solid yellow line* is the notch surface. *L*, lateral; *I*, inferior; *S*, superior; *M*, medial.

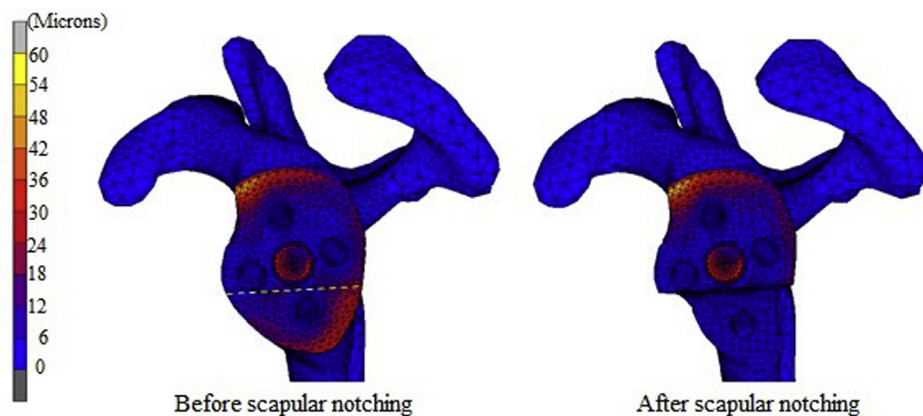


Figure 8 Distribution of bone-prosthesis micromotion before and after scapular notching. The *dotted yellow line* marked on the intact bone-prosthesis contact surface is the position of the notch surface that will be created later.

Grassi et al.¹¹ Screw fracture was possibly caused by the movement of the humeral component into the notch and the impact to the inferior screw.²³ It also may be induced by the stress concentration in the inferior screw thread, reducing the screw fatigue life. Generally, the inferior screw is comparatively safe even in the case of scapular notching.

However, if the inferior screw breaks, the root of the screw cap and the bone-notch interface are the regions at potentially high risk.

The maximum principal stresses on the surface of the inferior screw hole after scapular notching were analyzed. The peak stress in the cancellous bone reached 3.3 MPa

(SD, 0.9 MPa). This value was lower than the regional ultimate strength (13-110 MPa)^{1,9,20} and failure strength (9-15 MPa)¹ of cancellous bone but was on the same level as the fatigue failure strength (3.6 MPa) of epiphyseal cancellous bone with a Young modulus of 400 MPa after 1 million cycles.¹⁷ This finding suggests that scapular notching may increase the risk of bone fracture close to the inferior screw hole and may explain the possible screw loosening in the presence of scapular notching, which were reported to cover 40% of glenoid loosening.²⁶

Micromotions at the bone-prosthesis interface were analyzed to assess the effects of a severe inferior scapular notch on the initial stability of the glenoid component in RTSA. The results showed that few variations (2.68 μm [SD, 0.57 μm]) in notch-induced bone-prosthesis micromotions were observed after scapular notching. The maximum predicted bone-prosthesis micromotion of the implanted scapula accompanied by a severe scapular notch was 59.80 μm , which is on the same level as the threshold for bone ingrowth (50 μm)²² and predicted a generally effective bone-prosthesis environment for bone osseointegration. This finding was in line with the report of Nyffeler et al,²¹ in which a Delta III RTSA in the scapula retrieved at 8 months' follow-up, accompanied by a grade 3 inferior notch, was generally well supported by the bone biological attachments.

There are several limitations to our study. First, the unavoidable inconsistencies in the notch geometries and the positions of the glenoid prosthesis and screw fixations, as well between the experiment and the FEM, limit the precision of statistical comparison. The FEMs of 3 cadaveric scapulae in the intact condition were validated against results from in vitro cadaveric testing in our previous work.³⁰ Moreover, the differences between the FE predicted notch-induced variations in inferior screw stress and those from experiments were much smaller than the fatigue strength of the titanium screw material. The FE-experimental variations in bone-prosthesis micromotions were also much lower than the threshold for bone ingrowth. Therefore, the FEM of a scapula accompanied by an inferior notch can produce a result consistent with the reality. Second, only a severe inferior notch (Nerot-Sirveaux grade 4) was used in this study, although scapular notches are also observed in the anterior and posterior scapulae.²⁵ Because an inferior notch is one of the most significant regarding bone loss and because screw fractures were reported to be associated with the inferior scapular notch in the clinic,^{11,26} a severe inferior scapular notch is appropriate in assessing implant fixation. Third, the assessment of bone fracture was limited by the use of the fatigue failure value from bovine cancellous bone with a Young's modulus of 400 MPa.¹⁷ A proper fatigue failure limitation from scapular trabecular bone in daily life would improve the accuracy of our assessment. Finally, the use of LVDTs precluded the ability to measure the relative bone-prosthesis movement in the inferior glenoid. Future iterations of this test paradigm may use

slightly different motion capture techniques (eg, laser extensometer) to capture the displacements in all the regions around the glenoid.

Conclusion

This study was conducted to investigate the relationship between scapular notching and glenoid fixation in Grammont RTSA. Both the in vitro testing and FEM results presented few notch-induced variations in bone-prosthesis micromotions. The stress values along the inferior titanium screw in the implanted scapula accompanied by an inferior notch were lower than the screw fatigue strength and documented that the inferior screw was comparatively safe even in the presence of a severe inferior notch on the scapular neck. These findings may explain the long-term longevity of RTSA in the case of severe scapular notching. The relationship between the inferior scapular notch and the weak regions along the inferior screw (the root of the screw cap and the screw-notch conjunction) may explain why fractures of the inferior screw are sometimes reported in patients with RTSA clinically.

Acknowledgments

The authors thank Dr. Kontaxis from Newcastle University for the provision of force data for the Delta reverse shoulder arthroplasty in physiological daily activities.

Disclaimer

The authors, their immediate families, and any research foundations with which they are affiliated have not received any financial payments or other benefits from any commercial entity related to the subject of this article.

Supplementary data

Supplementary data to this article can be found online at <https://doi.org/10.1016/j.jse.2020.01.087>.

References

1. Anglin C, Tolhurst P, Wyss UP, Pichora DR. Glenoid cancellous bone strength and modulus. *J Biomech* 1999;32:1091-7.
2. Boileau P. Grammont reverse prosthesis: design, rationale, and biomechanics. *J Shoulder Elbow Surg* 2005;14:147-61. <https://doi.org/10.1016/j.jse.2004.10.006>

3. Carter DR, Hayes WC. The compressive behaviour of bone as a two-phase porous structure. *J Bone Joint Surg Am* 1977;59:954-62.
4. Chong D. Biomechanical analysis of fixation and bone remodelling of total knee replacement [PhD thesis]. London: Imperial College; 2009.
5. Chou J, Malak SF, Anderson IA, Astley T, Poon PC. Biomechanical evaluation of different designs of glenospheres in the SMR reverse total shoulder prosthesis: range of motion and risk of scapular notching. *J Shoulder Elbow Surg* 2009;18:354-9. <https://doi.org/10.1016/j.jse.2009.01.015>
6. Dabestani M. In vitro strain measurement in bone. In: Miles AW, Tanner KE, editors. *Strain measurement in biomechanics*. London: Chapman & Hall; 1992. p. 58-69.
7. Edwards TB, Trappey GJ, Riley C, O'Connor DP, Elkousy HA, Gartsman GM. Inferior tilt of the glenoid component does not decrease scapular notching in reverse shoulder arthroplasty: results of a prospective randomized study. *J Shoulder Elbow Surg* 2012;21:641-6. <https://doi.org/10.1016/j.jse.2011.08.057>
8. Ernstbrunner L, Andronic O, Grubhofer F, Camenzind RS, Wieser K, Gerber C. Long-term results of reverse total shoulder arthroplasty for rotator cuff dysfunction: a systematic review of longitudinal outcomes. *J Shoulder Elbow Surg* 2019;28:774-81. <https://doi.org/10.1016/j.jse.2018.10.005>
9. Farshad M, Gerber C. Reverse total shoulder arthroplasty—from the most to the least common complication. *Int Orthop* 2010;34:1075-82. <https://doi.org/10.1007/s00264-010-1125-2>
10. Favard L, Levigne C, Nerot C, Gerber C, De Wilde L, Mole D. Reverse prostheses in arthropathies with cuff tear: are survivorship and function maintained over time? *Clin Orthop Relat Res* 2011;469:2469-75. <https://doi.org/10.1007/s11999-011-1833-y>
11. Frich LH, Jensen NC, Odgaard A, Pedersen CM, Søjbjerg JO, Dalstra M. Bone strength and material properties of the glenoid. *J Shoulder Elbow Surg* 1997;6:97-104.
12. Gerber C, Canonica S, Catanzaro S, Ernstbrunner L. Longitudinal observational study of reverse total shoulder arthroplasty for irreparable rotator cuff dysfunction: results after 15 years. *J Shoulder Elbow Surg* 2018;27:831-8. <https://doi.org/10.1016/j.jse.2017.10.037>
13. Grassi FA, Murena L, Valli F, Alberio R. Six-year experience with the Delta III reverse shoulder prosthesis. *J Orthop Surg (Hong Kong)* 2009;17:151-6. <https://doi.org/10.1177/230949900901700205>
14. Gruber S, Schoch C, Geyer M. The reverse shoulder arthroplasty Delta Xtend: mid-term results. *Der Orthopade* 2017;46:222-6. <https://doi.org/10.1007/s00132-016-3355-5>
15. Harman M, Frankle M, Vasey M, Banks S. Initial glenoid component fixation in “reverse” total shoulder arthroplasty—a biomechanical evaluation. *J Shoulder Elbow Surg* 2005;14:162S-7S. <https://doi.org/10.1016/j.jse.2004.09.030>
16. Hopkins AR, Hansen UN, Bull AMJ, Emery R, Amis A. Fixation of the reversed shoulder prosthesis. *J Shoulder Elbow Surg* 2008;17:974-80. <https://doi.org/10.1016/j.jse.2008.04.012>
17. Kontaxis A. Biomechanical analysis of reverse anatomy shoulder prosthesis [PhD thesis]. Newcastle: Newcastle University; 2010.
18. Lévine C, Garret J, Boileau P, Alami G, Favard L, Walch G. Scapular notching in reverse shoulder arthroplasty. *J Shoulder Elbow Surg* 2008;17:925-35. <https://doi.org/10.1016/j.jse.2008.02.010>
19. Michel MC, Guo X-DE, Gibson LJ, McMahon TA, Hayes WC. Compressive fatigue behavior of bovine trabecular bone. *J Biomech* 1993;26:453-63.
20. Mimar R, Limb D, Hall RM. Evaluation of the mechanical and architectural properties of glenoid bone. *J Shoulder Elbow Surg* 2008;17:336-41. <https://doi.org/10.1016/j.jse.2007.07.024>
21. Nyffeler RW, Werner CM, Simmen BR, Gerber C. Analysis of a retrieved delta III total shoulder prosthesis. *Bone Joint J* 2004;86:1187-91. <https://doi.org/10.1302/0301-620x.86b8.15228>
22. Pilliar RM, Lee JM, Maniopoulos C. Observations on the effect of movement on bone ingrowth into porous-surfaced implants. *Clin Orthop Relat Res* 1986;208:108-13.
23. Roberts CC, Ekelund AL, Renfree KJ, Liu PT, Chew FS. Radiologic assessment of reverse shoulder arthroplasty. *Radiographics* 2007;27:223-35. <https://doi.org/10.1148/rg.271065076>
24. Roche CP, Stroud NJ, Martin BL, Steiler CA, Flurin P-H, Wright TW, et al. The impact of scapular notching on reverse shoulder glenoid fixation. *J Shoulder Elbow Surg* 2013;22:963-70. <https://doi.org/10.1016/j.jse.2012.10.035>
25. Simovitch RW, Zumstein MA, Lohri E, Helmy N, Gerber C. Predictors of scapular notching in patients managed with the delta III reverse total shoulder replacement. *J Bone Joint Surg Am* 2007;89:588-600. <https://doi.org/10.2106/JBJS.F.00226>
26. Sirveaux F, Favard L, Oudet D, Huquet D, Walch G, Mole D. Grammont inverted total shoulder arthroplasty in the treatment of glenohumeral osteoarthritis with massive rupture of the cuff: results of a multicentre study of 80 shoulders. *Bone Joint J* 2004;86:388-95. <https://doi.org/10.1302/0301-620x.86b3.14024>
27. Terrier A, Reist A, Merlini F, Farron A. Simulated joint and muscle forces in reversed and anatomic shoulder prostheses. *Bone Joint J* 2008;90:751-6. <https://doi.org/10.1302/0301-620X.90B6>
28. Wright T, Robert F, Closkey J. Properties of biomaterials used in joint replacements. In: Shanbhag A, Rubash H, Jacobs J, editors. *Joint replacement and bone resorption pathology, biomaterials, and clinical practice*. New York: Taylor & Francis Group; 2006. p. 123-45.
29. Wright TM, Hayes WC. Strain gage application on compact bone. *J Biomech* 1979;12:471-5.
30. Zhang M. Effects of scapular notching and bone remodelling on long-term fixation of the glenoid component in reverse shoulder arthroplasty [PhD thesis]. London: Imperial College; 2012.
31. Zhang M, Junaid S, Gregory T, Hansen U, Cheng C-K. Effect of baseplate positioning on fixation of reverse total shoulder arthroplasty. *Clin Biomech* 2019;62:15-22. <https://doi.org/10.1016/j.clinbiomech.2018.12.021>